Experimental Investigation of Rotorcraft Hub and Shaft Fairing Drag Reduction

Larry A. Young*, David R. Graham*, and Robert H. Stroub*
NASA Ames Research Center, Moffett Field, California

A wind-tunnel test was conducted to obtain data on several rotorcraft hub- and shaft-fairing drag reduction configurations. Aerodynamic loads and moments were acquired for each test configuration. All hub and shaft-fairing configurations were tested on a 1/5-scale XH-59A model fuselage. Both coaxial- and single-rotor configurations were tested, and all rotor assemblies were modeled with nonrotating hardware. The drag reduction methods tested included cambered elliptical hub fairings, several different shaft fairings, and strakes. Test data show that significant drag reductions can be attained with certain fairing configurations. The lowest drag values for the single rotor configurations were obtained for a cambered elliptical hub fairing with a large thickness airfoil shaft fairing. The lowest coaxial-configuration drag values were obtained with cambered elliptical hub fairings and a long chord intermediate shaft fairing.

Nomenclature

C_d = drag coefficient, based on projected frontal area, $D/(qA)$
D = model drag, N
D_f = fuselage effective diameter for the cross-sectional cut at the rotor shaft centerline, m
d = planform diameter of the hub fairings, where d_e is the elliptical hub-fairing diameter, m
h = shaft/shaft-fairing height, m
q = tunnel dynamic pressure, N/m
t = hub-fairing maximum thickness, m
t_{sf} = a shaft-fairing maximum thickness, m
α = helicopter model fuselage angle of attack, positive nose up, deg
ΔD = incremental drag, drag of fairings and fuselage minus the fuselage only drag, N
θ_i = horizontal strake incidence angle, positive noseup, deg

Introduction

HUB and shaft drag contributes 20–50% of the total drag of a rotorcraft. Concern over helicopter cruise efficiency has increased as cruise speeds and fuel costs have increased. Substantial fuel savings could result from reductions in this drag component. For example, Ref. 1 studied the potential fuel savings that would result from incremental improvements in reducing helicopter drag. An estimated 13% fleetwide fuel cost savings would occur for a 50% hub-drag reduction implemented on 36% of the civilian helicopter fleet.

References 2–4 provide extensive documentation from previously proposed methods for reduction of hub and shaft drag. Among the methods proposed and /or explored are area rule pylon fairings, hub fairings, blade-shank fairings, shaft fairings, boundary-layer flow control, and strakes. These drag reduction methods have been only partially incorporated into the newer rotorcraft designs. Because of the current helicopter speeds and ranges, the drag reductions obtained from fairing configurations must be substantial to justify the additional complexity, weight, and maintenance penalties of implementing the fairings.

A small-scale wind-tunnel test was conducted at Ames Research Center (ARC) to investigate several new drag reduction configurations. This test was to identify promising low drag hub- and shaft-fairing configurations for both coaxial- and single-rotor helicopters. Only nonrotating hub fairings were tested because the difference in drag values between nonrotating and rotating hub fairings was assumed to be small. This assumption is supported by the test results reported in both Refs. 4 and 5. The purpose of this paper is to summarize the results of this drag reduction wind-tunnel test.

Description of Apparatus

The baseline helicopter model is shown in Fig. 1 as installed in the ARC Army 7 × 10-ft wind tunnel. The fuselage is a 1/5-scale XH-59A model without the auxiliary propulsion. The model was sting-mounted on its side on the external balance of the wind tunnel. Model angle-of-attack changes were performed by yawing the tunnel turntable, and the model was tested at zero yaw.

The hub and shaft assembly models are organized into three groups: single-rotor hub and shaft fairings, single-rotor strakes, and coaxial- rotor hub and shaft fairings. Figures 2–13 show the tested model drag reduction configurations for both single- and coaxial-rotor hub and shaft assemblies. The important geometrical parameters of each configuration will be noted below.

Single-Rotor Hub and Shaft Fairings

Figures 2 and 3 show the two hub fairings tested with an unfaired shaft assembly. Figure 2 is a photograph of the test baseline single-rotor hub fairing and shaft assembly. This baseline configuration consisted of a 24% t/d elliptical hub fairing and an unfaired shaft with simulated swash plate and control rods. The hub-fairing maximum thickness was 0.07m. The surface curvature of the fairing was defined by a circular arc. The shaft height was 0.18m giving a h/D_f ratio of 0.41, and the shaft diameter was 0.2 d_e. The swash plate was fixed and not tilted with respect to the shaft and had a diameter of 0.54 d_e. An 18% t/d cambered elliptical fairing was tested and is shown in Fig. 3. The cambered elliptical fairing's maximum

Presented as Paper 86-1783 at the AIAA Applied Aerodynamics Conference, San Diego, June 9–11, 1986; received July 30, 1986; revision received Jan 20, 1987.

*Aerospace Engineer.

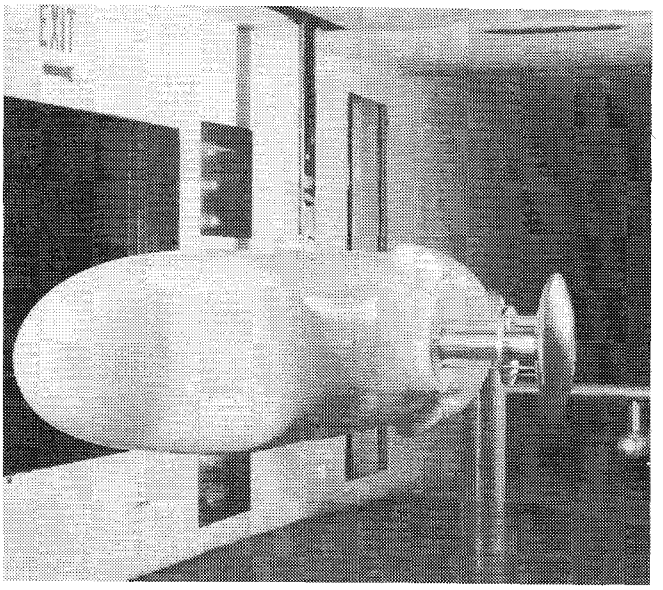

Fig. 1 1/5 scale helicopter model with single-rotor configuration.

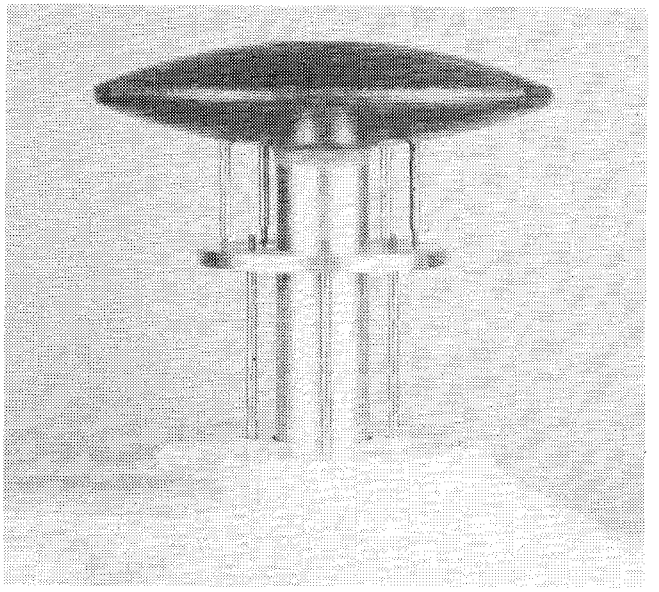

Fig. 2 Single-rotor elliptical hub fairing with unfaired shaft assembly.

thickness, upper surface curvature, and edge radius were the same as for the baseline elliptical hub fairing's, yet the cambered elliptical hub-fairing lower surface was a flat plane.

Figures 4–8 show the five shaft fairings tested for the single-rotor fairing configurations: circular arc fairing, 0012 dual-component fairing, baseline fairing, teardrop fairing, and the large thickness airfoil fairing. All five shaft fairings were tested with the elliptical hub fairing. Shaft fairing height was not varied in the test, and there were no gaps between the hub and shaft fairings. The cambered elliptical hub fairing was tested with three shaft fairings (the circular arc fairing, the 0012 dual-component fairing, and the large thickness airfoil fairing).

Figure 8 also shows the modifications made to a large thickness airfoil-type shaft fairing. The modifications consisted of rounding the fairing nose to a leading-edge radius of 0.42 t_{sf} and the removal of trailing-edge wedges of 10 deg slope each. Three hub fairings were tested with the shaft fairing modifications. In addition to the baseline elliptical hub fairing and the 18% t/d cambered elliptical hub fairing, a 33% t/d cambered elliptical hub fairing was tested. The 33% t/d cambered hub fairing had a 0.127 m maximum thickness, a circular arc upper surface, and a flat lower surface.

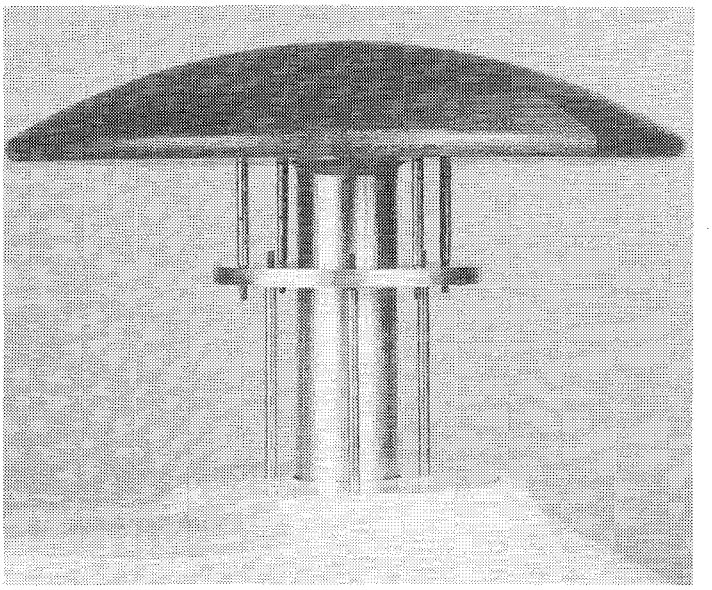

Fig. 3 Single-rotor cambered elliptical hub fairing with unfaired shaft assembly.

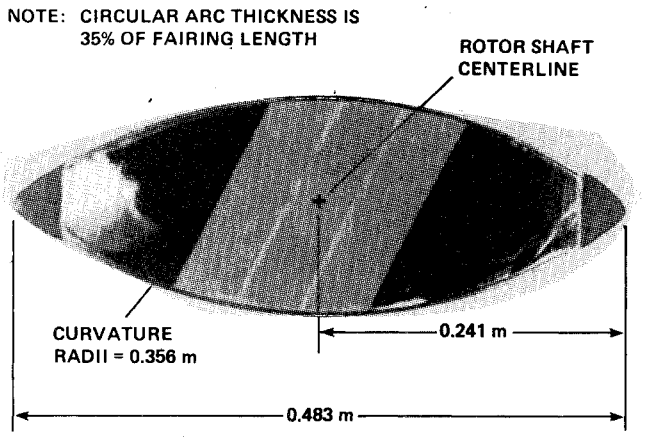

Fig. 4 Circular arc shaft fairing.

Single-Rotor Strakes

Figure 9 and 10 show vertical and horizontal strakes placed aft of the unfaired rotor-shaft assembly. The strakes were tested with the 24% t/d elliptical hub fairing. The vertical strake configuration was tested at two different lateral strake positions: one where the vertical strakes were laterally spaced apart by 0.05 m (0.18d_e) and the other with 0.11 m (0.39d_e) spacing. The longitudinal location of the leading edges of the vertical strakes was 0.36 d_e aft of the rotor shaft centerline. The vertical strakes were held into place by an upper and lower base plate. The vertical strakes had a thickness-to-chord ratio of 12% and a chord length of 0.051 m. The contours roughly approximated a symmetrical airfoil. For both strake spacings, each vertical strake was set at a positive lateral incidence angle of 7 deg. A horizontal strake configuration was tested with the strake incidence angle set at three different angles: 0, 5, and 10 deg. The longitudinal location of the leading edge of the horizontal strake was 0.31 d_e aft of the rotor shaft centerline. The horizontal strake was essentially a flat plate with a chord length of 0.102 m.

Coaxial-Rotor Hub and Shaft Fairings

Figures 11–13 show the tested coaxial-rotor hub and shaft fairing configurations. Figure 11 shows a simulated coaxial

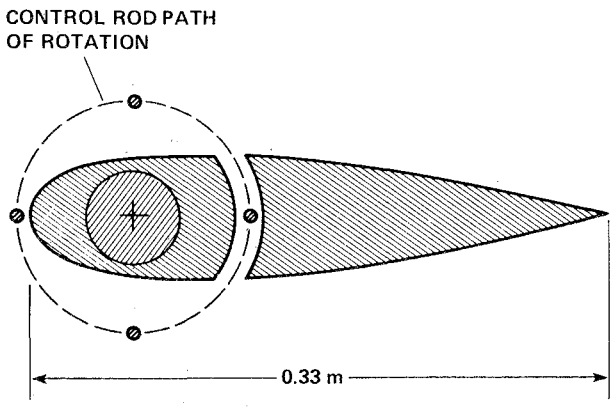

Fig. 5 0012 dual-component shaft fairing.

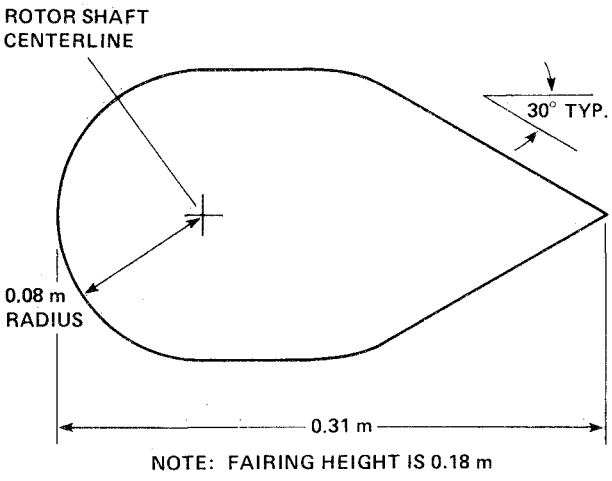

Fig. 6 Baseline shaft fairing.

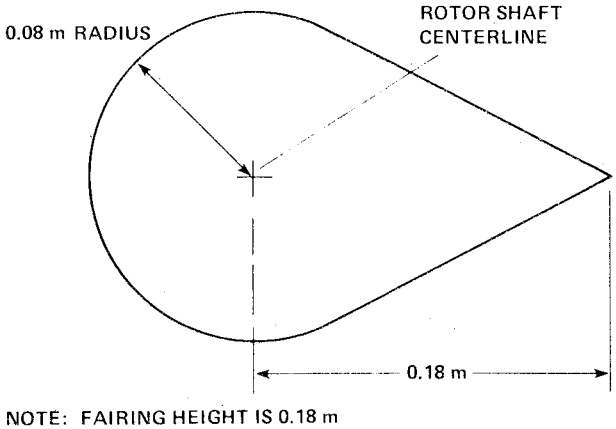

Fig. 7 Teardrop shaft fairing.

unfaired hub and shaft that was tested. Figure 12 shows the baseline faired coaxial configuration, which consisted of two elliptical hub fairings and a short chord airfoil intermediate shaft fairing. The coaxial hub fairings had the same dimensions as the single-rotor elliptical hub fairing. The short chord shaft fairing maximum thickness was 0.07 m, and it had a 40% thickness-to-chord ratio. The elliptical hub fairings were also tested with a long chord shaft fairing. The long chord shaft fairing had the same maximum thickness as the shorter fairing and a 27% thickness-to-chord ratio.

Two cambered elliptical coaxial hub-fairing configurations were tested: configuration 1 is shown in Fig 13a and configuration 2 in Fig. 13b. Both the upper and lower cambered

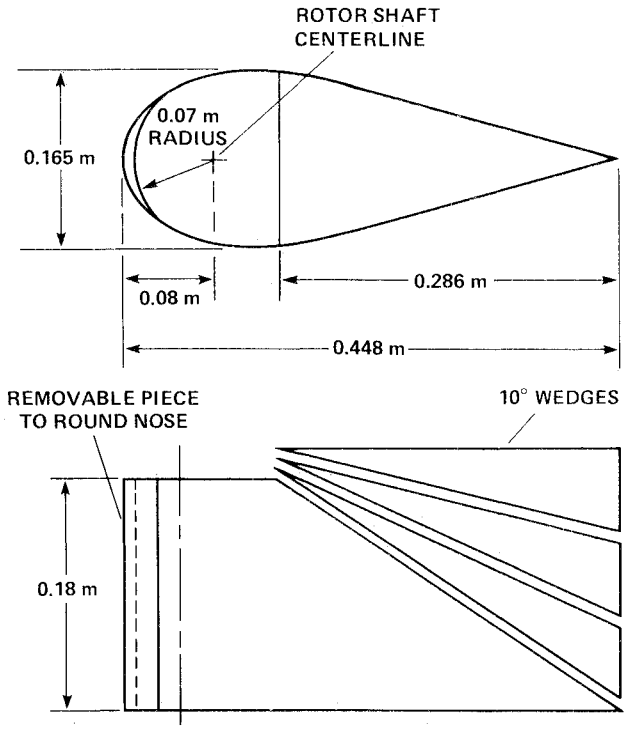

Fig. 8 Large thickness airfoil shaft fairing and tested modifications.

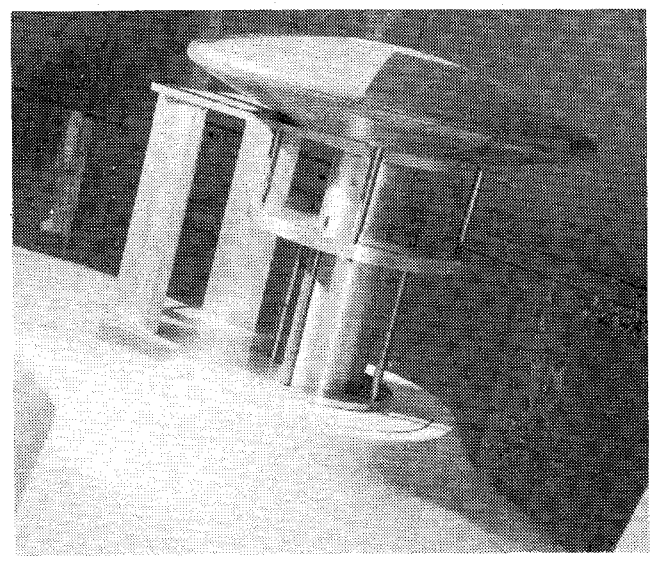

Fig. 9 Single-rotor vertical strakes.

elliptical fairings had the same dimensions as the single-rotor 18% t/d cambered elliptical hub fairing. Though not shown, a combined elliptical and cambered-elliptical fairing configuration was tested with the long chord shaft fairing.

Test Procedures

Model six-component forces and moments were acquired for all configurations tested. Data were typically acquired at a tunnel dynamic pressure of 3830 N/m. The tunnel Mach number was 0.23; the Reynolds number per unit-length was $5.01 \times 10^6 m^{-1}$; the tunnel velocity was approximately 79 m/s. Model angle of attack sweeps were performed from +2 to -8.

Results

All model drag measurements were normalized by tunnel dynamic pressure. Sting tares have been subtracted from the

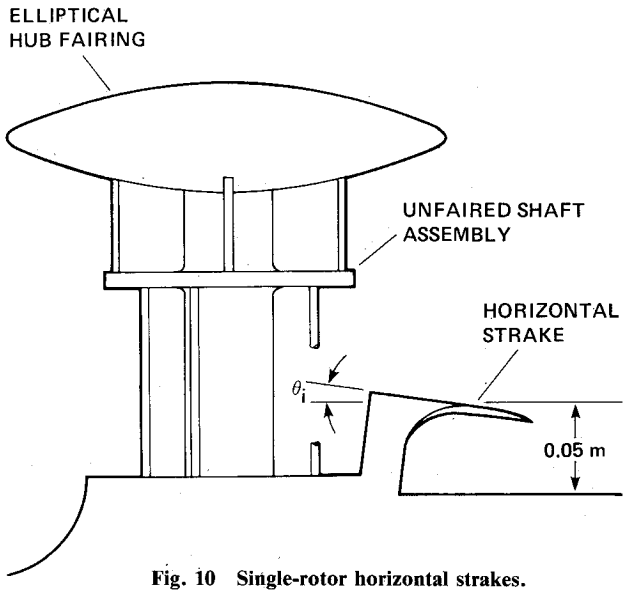

Fig. 10 Single-rotor horizontal strakes.

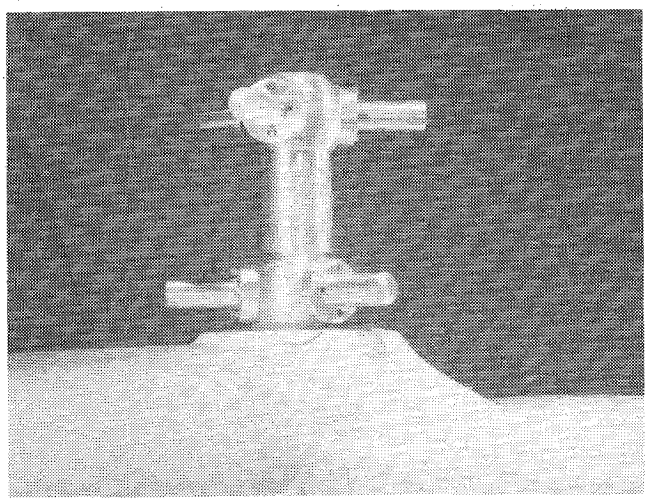

Fig. 11 Simulated coaxial unfaired hubs and shaft.

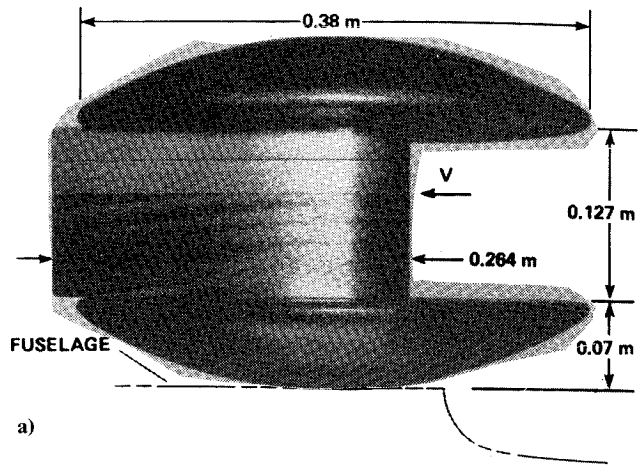

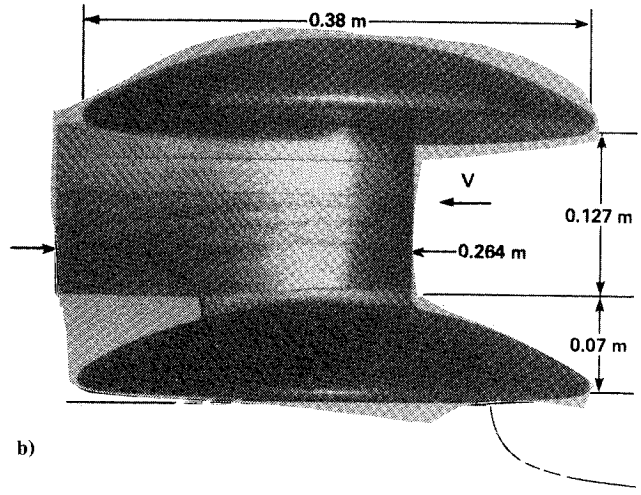

Fig. 13 Cambered coaxial hub fairing configurations: a) with an elliptical hub fairing and b) with a cambered elliptical hub fairing.

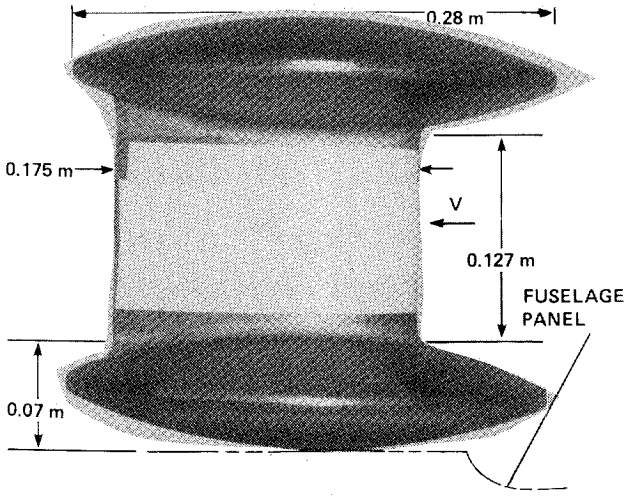

Fig. 12 Coaxial elliptical hub fairings and short chord shaft fairing.

test data. Averaged data points were taken for each model angle of attack and dynamic pressure. Each average point is based on three test points with twenty samples. The blockage of the fuselage at $\alpha = 0$ was approximately 2.5%. Blockage corrections were not made to the tunnel dynamic pressure values. Drag measurements for the model configurations tested are presented in Figs. 14–19. The model drag values are estimated to have an accuracy of approximately $8.7 \times 10^{-4} m^2$, based on repeat run data.

Single-Rotor Hub and Shaft Fairings

Figures 14a and 14b are plots of D/q vs α for several single-rotor shaft fairings, for both the elliptical and cambered elliptical hub fairings. A number of shaft fairings, for a given hub fairing, resulted in substantial drag reductions, approximately 40–50% less incremental drag than with the unfaired shaft assembly. The low drag shaft fairings were the circular arc fairing (defined in Fig. 4), the large thickness airfoil shaft fair-

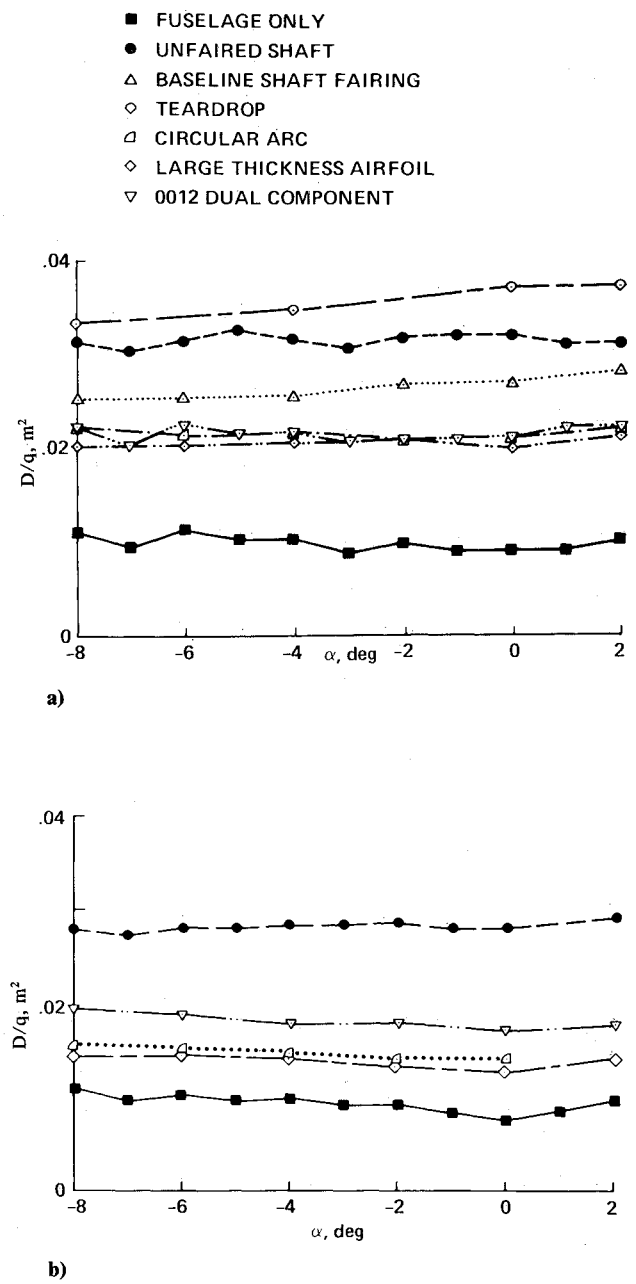

Fig. 14 *D/q* comparisons between single-rotor shaft fairings: a) with an elliptical hub fairing and b) with a cambered elliptical hub fairing.

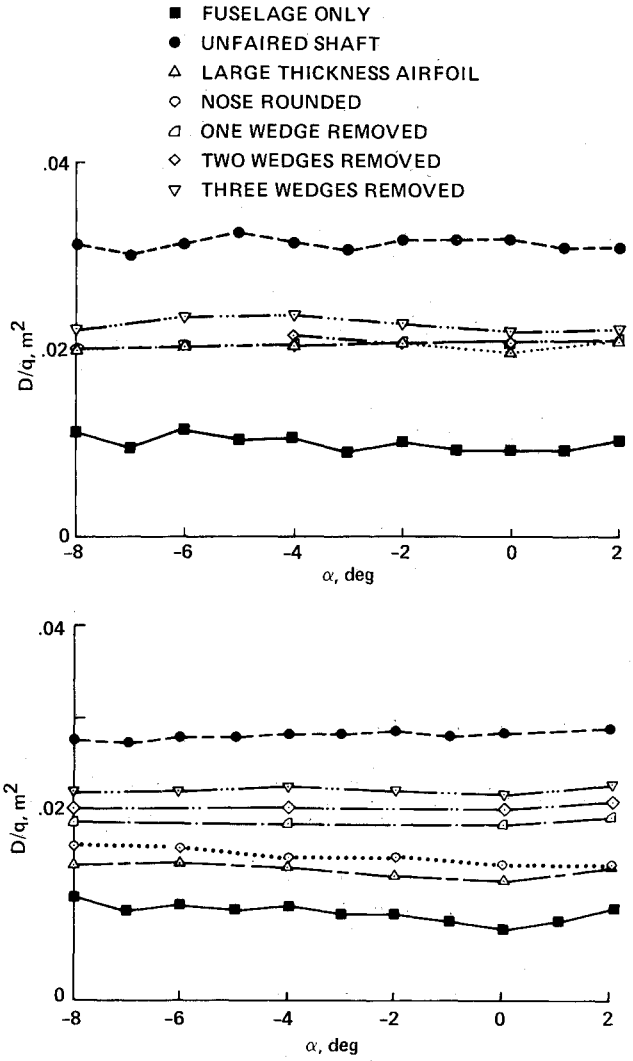

Fig. 15 *D/q* comparisons of large thickness airfoil shaft fairing modifications.

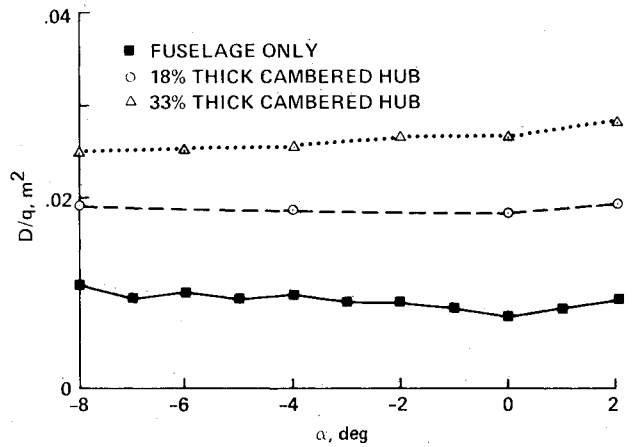

Fig. 16 *D/q* comparison between 18% and 33% *t/d* cambered elliptical hub fairings with modified large thickness airfoil shaft fairing.

ing (defined in Fig. 8), and the 0012 dual-component fairing (defined in Fig. 5). Each of these three shaft fairings, when tested with the 18% *t/d* cambered elliptical hub fairing, had less drag than the same shaft fairing with the elliptical hub fairing. Additionally, the model drag demonstrated increased sensitivity to shaft fairing shape for configurations with the cambered elliptical hub fairing than with the elliptical fairing. Finally, when compared to a high-drag fairing configuration (which was the elliptical hub fairing and the unfaired shaft), the minimum-drag configuration (the cambered hub fairing and the large thickness airfoil shaft fairing) resulted in an approximately 70% incremental drag reduction.

Figures 15a and 15b are plots of D/q vs α for various large thickness airfoil shaft fairing leading and trailing edge modifications (modifications are illustrated in Fig. 8). Rounding the nose of the shaft fairing resulted in little change in drag. Modifying the trailing edge of the shaft fairing by removing 10 deg wedges resulted in small drag increases for the elliptical hub fairing configurations. Trailing-edge shaft fairing modifications resulted in substantial drag increases for the cambered hub fairing configurations, especially with the removal of the first wedge. Therefore, this would suggest that shaft fairing trailing edges should not be sloped but that the fairing should be kept rectangular in planform.

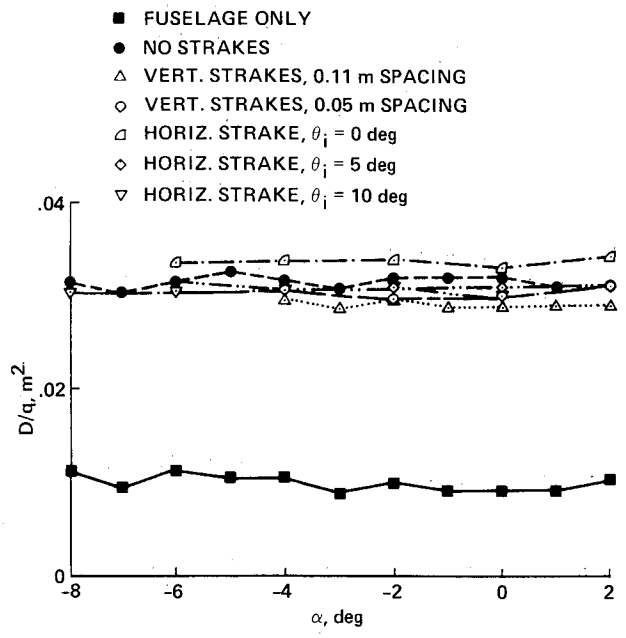

Fig. 17 *D/q* **comparisons between single-rotor strake configurations.**

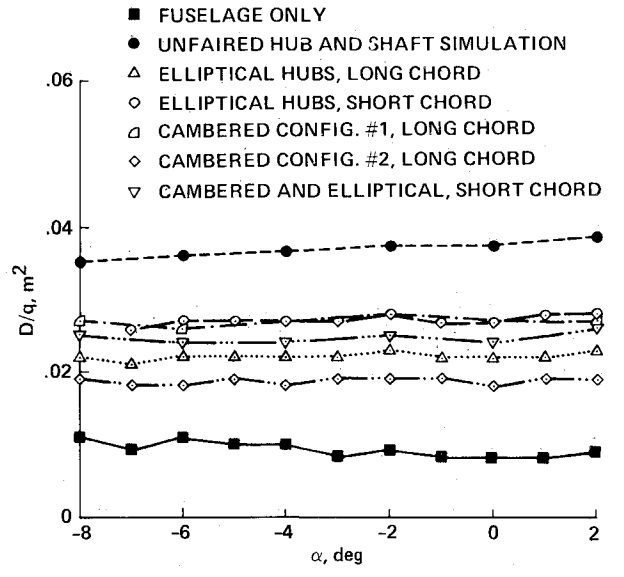

Fig. 18 *D/q* **comparison between coaxial fairing configurations.**

Figure 16 shows a direct comparison of D/q values for the two cambered elliptical hub fairings tested with the large thickness airfoil shaft fairing, modified with one wedge removed from the trailing edge. The 33% thick hub fairing has nearly twice the average incremental D/q of the 18% thick hub fairing. C_d values for the combined hub and shaft fairing configurations were calculated. The C_d value of the 18% thick cambered hub with the modified large thickness airfoil shaft fairing is 0.20. The C_d value for the 33% thick cambered elliptical hub fairing with the modified shaft fairing is 0.28.

Single-Rotor Strakes

Figure 17 is a plot of D/q vs α for the single-rotor unfaired shaft assembly with both vertical and horizontal strakes. Very small drag improvements were seen by adding strakes to the model. The minimum drag strake was the vertical strake with 0.11 m spacing, which resulted in a 5–10% drag improvement. The horizontal strake (with incidence angles of 0 and 5 deg) had slightly less drag than the no-strake baseline. The horizontal strake at an incidence angle of 10 deg had more drag than the no-strake baseline.

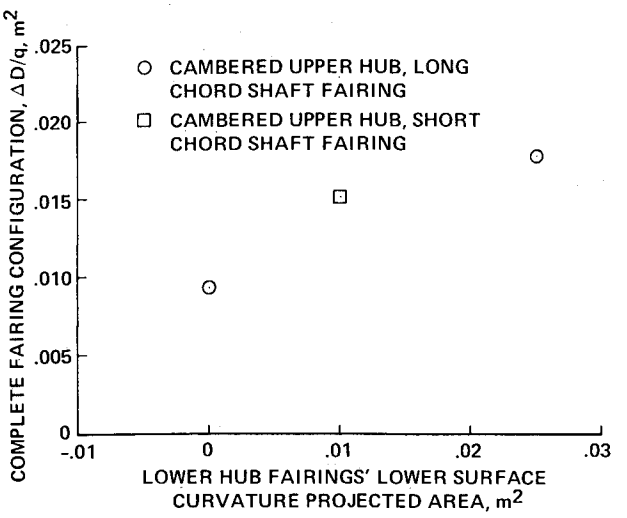

Fig. 19 Dependence of coaxial fairing configurations $\Delta D/q$ on lower hub fairing lower surface projected area.

Coaxial-Rotor Hub and Shaft Fairings

Figure 18 is a plot of D/q vs α for several coaxial hub and shaft fairing configurations. The minimum drag coaxial configuration is the cambered elliptical hub fairing configuration 2 (defined in Fig 13b), which has an incremental drag 50% less than the elliptical hub fairing configuration (defined in Fig. 12).

Three drag mechanisms contribute to the cambered hub-fairing configuration 2 low D/q values. First, the smaller thickness-to-chord ratio of the long chord shaft fairing will result in a smaller D/q than the short chord shaft fairing. Second, the flat plane of the upper cambered elliptical hub fairing prolongs steady flow on the shaft fairing. Third, the wake generated at the base of the lower cambered hub fairing produces a negative pressure region aft of the fairing that contributes less to the fairing pressure drag than an elliptical lower fairing. This wake induced pressure drag component depends in part on two characteristics of the lower hub fairing lower surface. These two characteristics are the surface area size and the surface curvature, both of which determine the projected area on which the negative pressure distribution acts to produce drag.

The limited experimental data of Fig. 19 agree with the wake-induced pressure drag mechanism hypothesis by demonstrating a dependency of fairing drag on the lower hub fairing lower surface geometry, as represented by the projected area estimate of that surface. A future coaxial hub fairing test objective should be the acquisition of a data set of fairing surface pressures to quantify pressure drag as a function of hub fairing camber and surface geometry.

The present test coaxial-rotor low-drag hub and shaft fairings were compared in a limited way to previous small-scale test results by retesting the Ref. 6 "advanced configuration" (model designation A3A4S6) fairings during this test. The Ref. 6 hub fairings were approximately elliptical with a diameter of 0.241 m and a maximum thickness of 0.044 m. The data of the retested A3A4S6 fairings are in good agreement with the original Ref. 6 drag data; both show the $\Delta D/q$ to be approximately 0.011m.

The present test minimum-drag cambered elliptical hub-fairing configuration 2 has approximately the same $\Delta D/q$ as the advanced configuration from Ref. 6. However, the coaxial fairing configurations studied during this test were based upon the 1/5-scale dimensions of the XH-59A hub and shaft assembly, whereas the Ref. 6 advanced fairing configuration was sized for a smaller coaxial rotor system. Therefore, the advantage of this test's minimum-drag coaxial fairings over the Ref. 6 fairings becomes apparent when a drag coefficient comparison is made. The C_d of the minimum-drag coaxial

cambered fairing configuration is 0.23, whereas the C_d for the Ref. 6 advanced configuration fairing was only 0.43.

Summary of General Fairing Characteristics

1) For single-rotor fairing configurations, the cambered elliptical hub fairing has general applicability for reducing drag.

2) Single-rotor shaft fairing contour shape is an important factor in reducing drag when used with the cambered elliptical hub fairing.

3) The planform shape of shaft fairings is an important factor in reducing drag when used with the cambered elliptical hub fairing. Going from a rectangular shaft fairing planform to one with a sloped trailing edge increases the drag considerably.

4) Tested strakes for single-rotor configurations did not result in large drag reductions, but they could perhaps be used in conjunction with hub and shaft fairings to make small to moderate improvements.

5) Reducing the thickness-to-chord ratio of the intermediate shaft fairing for coaxial fairing configurations result in substantial reductions in drag. In order to reduce the thickness ratio, it is necessary to increase the shaft fairing chord length and the diameters of the hub fairings.

6) Coaxial fairing configurations having hub fairings with flat planes for lower surfaces result in substantial drag reductions.

Conclusions

A number of hub and shaft fairings have been shown to have low drag values. These low drag fairings include several single-rotor shaft fairing configurations incorporating cambered elliptical hub fairing and a coaxial cambered elliptical hub and shaft fairing configuration. The minimum drag rotor hub fairing combination was the cambered hub fairing with the large thickness airfoil shaft fairing (Fig. 8). This single-rotor fairing configuration resulted in an approximately 70% less incremental drag than an elliptical hub fairing with unfaired shaft assembly. The minimum drag coaxial fairing configuration was the cambered elliptical hub-fairing configuration 2 (Fig. 13b), where the hub fairings had flat lower surfaces. This coaxial fairing combination resulted in a 50% incremental drag reduction as compared to elliptical hub fairings and a short chord shaft fairing.

References

[1]Stroub, R.H., and Rabbott J.P. Jr., "Wasted Fuel—Another Reason for Drag Reduction," Special Report, 31st AHS National Forum, Washington, DC, May 1975.

[2]Williams, R.M. and Montana P.S., "A Comprehensive Plan for Helicopter Drag Reduction," Special Report, 31st AHS National Forum, Washington, DC, May 1975.

[3]Keys, C.N. and Rosenstein, H.J., "Summary of Rotor Hub Drag Data," NASA CR-152080, March 1978.

[4]Montana, P.S., "Experimental Investigation of Three Rotor Hub Fairing Shapes," David W. Taylor Naval Ship Research and Development Center Rept. ASED 333, Bethesda, MD, May 1975.

[5]Felker, Fort F., "An Experimental Investigation of Hub Drag on the XH-59A," AIAA Paper 85-4065, Oct. 1985.

[6]Balch, D.T. and Weiner, S., "1/5 Scale ABC Hub Drag Test—Final Report," SER-69063, Contract NASA2-10215, March 1980.